

Theoretical Interpretation of Learned Step Size in Deep-Unfolded Gradient Descent

Satoshi Takabe*† and Tadashi Wadayama*

*Nagoya Institute of Technology, Gokiso, Nagoya, Aichi, 466-8555, Japan,

{wadayama, s_takabe}@nitech.ac.jp

†RIKEN Center for Advanced Intelligence Project, Chuo-ku, Tokyo, 103-0027, Japan

Abstract—Deep unfolding is a promising deep-learning technique in which an iterative algorithm is unrolled to a deep network architecture with trainable parameters. In the case of gradient descent algorithms, as a result of training process, one often observes acceleration of convergence speed with learned non-constant step size parameters whose behavior is not intuitive nor interpretable from conventional theory. In this paper, we provide theoretical interpretation of learned step size of deep-unfolded gradient descent (DUGD). We first prove that training processes of DUGD reduces not only the mean squared error loss but also the spectral radius regarding the convergence rate. Next, it is shown that minimizing an upper bound of the spectral radius naturally leads to the Chebyshev step which is a sequence of the step size based on Chebyshev polynomials. Numerical experiments confirm that Chebyshev steps qualitatively reproduce the learned step size parameters in DUGD, which provides a plausible interpretation of learned parameters. In addition, it is shown that Chebyshev steps achieve the lower bound of the convergence rate of the first order method in a specific limit without learning nor momentum terms.

I. INTRODUCTION

Deep unfolding [10], [12] is a promising deep-learning approach whose architecture is based on existing iterative algorithms with tuning parameters such as step sizes in gradient descent (GD). The recursive structure of the algorithm is unrolled to a deep network and some parameters are embedded to the network. These parameters can be trained by standard deep learning techniques such as back propagation and stochastic gradient descent if all processes of the algorithm is differentiable. One notable advantage of deep unfolding is the acceleration of the convergence speed by tuning parameters compared with the original algorithm. Embedding proper trainable parameters also offers a flexible network structure to the algorithm that is applicable, e.g., to inverse problems with/without prior information [26]. Since deep unfolding has been applied to iterative algorithms for compressed sensing [3], [15], [17], [35], [38], a number of deep unfolding-based algorithms are proposed in various fields such as image recovery [16], [18], [22], [25], [34], [40] and wireless communications [11], [27], [33], [36], [37], [39]. Recently, theoretical aspects of deep unfolding also have been investigated [5], [21], [23].

In order to demonstrate deep unfolding, let us consider a

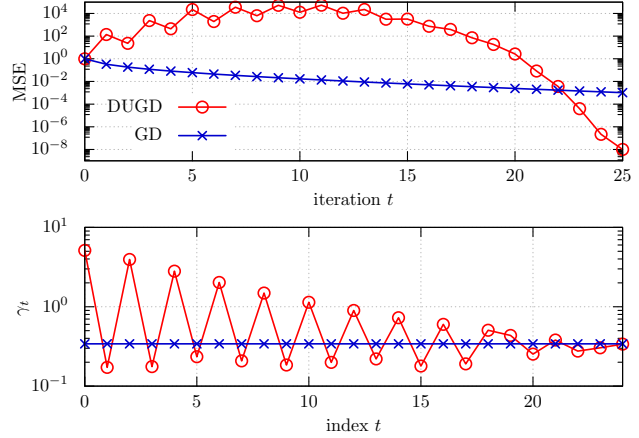


Fig. 1. MSE performance (upper) and learned step size parameters $\{\gamma_t\}_{t=0}^{24}$ (lower) of DUGD (circles) and GD with a constant step size (cross marks) when $(n, m) = (300, 600)$. The details of experimental conditions are written in Appendix A.

simple least mean square (LMS) problem written by

$$\hat{\beta} := \operatorname{argmin}_{\beta \in \mathbb{C}^n} \frac{1}{2} \|\mathbf{y} - \mathbf{H}\beta\|_2^2, \quad (1)$$

where $\mathbf{y} := \mathbf{H}\beta + \mathbf{n} \in \mathbb{C}^m$ is a measurement vector with noise vector \mathbf{n} and a measurement matrix $\mathbf{H} \in \mathbb{C}^{m \times n}$. Although the solution of (1) is explicitly given by $\hat{\beta} = (\mathbf{H}^* \mathbf{H})^{-1} \mathbf{H}^* \mathbf{y}$ ($m \geq n$) using Hermitian transpose matrix \mathbf{H}^* , GD is often used to reduce the computational complexity. The recursive formula of GD is given by

$$\beta^{(t+1)} = \beta^{(t)} - \gamma \mathbf{H}^* (\mathbf{y} - \mathbf{H}\beta^{(t)}) \quad (t = 0, 1, 2, \dots), \quad (2)$$

where $\beta^{(0)}$ is an initial vector and γ is a step size parameter. It is well known that the step size parameter controls the convergence speed of GD. The optimal value of γ is given by the largest and smallest eigenvalues of $\mathbf{H}^* \mathbf{H}$ in the LMS problem, and it is found heuristically in general.

Alternatively, we define deep-unfolded GD (DUGD) by

$$\beta^{(t+1)} = \beta^{(t)} - \gamma_t \mathbf{H}^* (\mathbf{y} - \mathbf{H}\beta^{(t)}), \quad (3)$$

where γ_t is a trainable step size parameter that depends on an iteration index t . The parameters $\{\gamma_t\}$ can be trained using a training data $\{(\tilde{\beta}^{[k]}, \tilde{\mathbf{y}}^{[k]})\}_k$ by minimizing a loss

function like mean squared error (MSE) $\|\tilde{\beta} - \beta^{(T)}\|_2^2/n$ between the estimate the output $\beta^{(T)}$ after T iterations and $\tilde{\beta}$. Figure 1 shows the empirical results of MSE performance (upper) and learned parameters $\{\gamma_t\}$ (lower) of DUGD and the original GD with the optimal constant step size when $(m, n) = (300, 600)$ (see Appendix A for details). We find that the learned parameter sequence exhibits a *zig-zag shape*, which accelerates convergence speed compared with a naive GD with a constant step size. These learned parameters are not intuitive nor interpretable from conventional theory. This kind of nontrivial step size parameters is observed not only DUGD but also other deep unfolding-based algorithms which contain a nonlinear projection step [15], [21]. As for an iterative soft thresholding algorithm for compressed sensing, it is proved that larger step sizes accelerate its convergence speed although finding proper step sizes is computationally hard in practice [1].

In this paper, the goal is to provide a plausible interpretation of learned parameters of DUGD and show that the parameters can accelerate the convergence speed of GD.

The contributions of this paper are listed as follows:

- It is shown that minimizing a MSE loss in DUGD reduces a spectral radius related to the convergence rate of GD. This suggests that properly learned step size parameters can accelerate the convergence speed.
- By minimizing an upper bound of the spectral radius, we derive Chebyshev steps that are a sequence of step sizes based on Chebyshev polynomials. Numerical experiments confirm that Chebyshev steps qualitatively reproduce the learned step size parameters in DUGD.
- Convergence analysis of GD with Chebyshev steps is executed, which reveals that Chebyshev steps improve the convergence speed. In addition, the convergence rate approaches to the lower bound of first order methods in a specific case even though it does not require a momentum term. Numerical results support the analysis and an application to ridge regression is demonstrated.

Related works: GD is a fundamental algorithm in continuous optimization [7]. GD is originally proposed by Cauchy [4], which is known as the steepest descent algorithm. The convergence rate of GD with a line search method including Cauchy's method is analyzed by Forsythe [8]. Acceleration of the convergence speed is a crucial issue in the literature. A well-known technique is the use of a momentum term. It is originated from the heavy ball method [30], which is simply called momentum method [32] in the machine learning community. Chebyshev semi-iterative method [9] and Nesterov's accelerated GD [28] are other algorithms using a momentum term. For convex quadratic problems, it is proved that these algorithms with momentum terms are optimal because their convergence rates are proportional to the lower bound of first order methods [20], [28]. In this paper, we treat GD with a step size sequence and without momentum terms that matches the recursive relation of DUGD.

II. DEEP-UNFOLDED GRADIENT DESCENT

In this paper, we consider a minimization of a convex quadratic function $f(\mathbf{x}) = \mathbf{x}^T \mathbf{A} \mathbf{x} / 2$ where $\mathbf{A} \in \mathbb{C}^{n \times n}$ is an Hermitian positive definite matrix, and $\mathbf{x}_{\text{opt}} = \mathbf{0}$ is its solution. Note that this minimization problem corresponds to the LMS problem (1) under a proper transformation.

The corresponding GD algorithm with a step size sequence $\{\gamma_t\}$ is given by

$$\mathbf{x}^{(t+1)} = (\mathbf{I}_n - \gamma_t \mathbf{A}) \mathbf{x}^{(t)} := \mathbf{W}^{(t)} \mathbf{x}^{(t)}, \quad (4)$$

where \mathbf{I}_n is the identity matrix of order n and $\mathbf{x}^{(0)}$ is an arbitrary point in \mathbb{C}^n .

In DUGD, we first fix the total number of iterations $T(\ll n)$ ¹ and train step size parameters $\{\gamma_t\}_{t=0}^{T-1}$. Training these parameters is usually executed by minimizing the MSE loss function $L(\mathbf{x}^{(T)}) := \|\mathbf{x}^{(T)} - \mathbf{x}_{\text{opt}}\|_2^2/n$ between the output $\mathbf{x}^{(T)}$ of DUGD and the true solution $\mathbf{x}_{\text{opt}} = \mathbf{0}$. In addition, to ensure convergence of DUGD, we assume that DUGD uses a learned parameter sequences $\{\tilde{\gamma}_t\}_{t=0}^{T-1}$ repeatedly for $t > T$. More specifically, in the t th iteration, we assume that $\gamma_t := \tilde{\gamma}_{t'}$ where $t' \equiv t \pmod{T}$. In this case, the output after every T steps is written by

$$\mathbf{x}^{((k+1)T)} = \left(\prod_{t=0}^{T-1} \mathbf{W}^{(t)} \right) \mathbf{x}^{(kT)} := \mathbf{Q}^{(T)} \mathbf{x}^{(kT)}, \quad (5)$$

for any $k = 0, 1, 2, \dots$. Note that $\mathbf{Q}^{(T)}$ is a function of step size parameters $\{\gamma_t\}_{t=0}^{T-1}$.

Our motivation is to show that a proper step size parameter sequence $\{\gamma_t\}$ accelerates the convergence speed of GD. In this setup, an asymptotic convergence speed can be measured by a spectral radius of a matrix $\mathbf{Q}^{(T)}$. Let τ_1, \dots, τ_n be the eigenvalues of a matrix $\mathbf{Q} \in \mathbb{C}^{n \times n}$. Then, the spectral radius of \mathbf{Q} is defined by

$$\rho(\mathbf{Q}) := \max_{i \in \{1, \dots, n\}} \{|\tau_i|\}. \quad (6)$$

For GD defined by (5), it converges to an optimal solution if $\rho(\mathbf{Q}^{(T)}) < 1$ holds. In addition, since the error between $\mathbf{x}^{(kT)}$ and the optimal solution is bounded by using $\rho(\mathbf{Q}^{(T)})$, the spectral radius indicates the asymptotic convergence rate of the algorithm.

III. THEORETICAL ANALYSIS

In this section, we will show the following three facts: (i) minimizing the MSE loss in DUGD also reduces the spectral radius $\rho(\mathbf{Q}^{(T)})$, (ii) a step size parameter sequence defined by an explicit form minimizes the upper bound of spectral radius $\rho(\mathbf{Q}^{(T)})$, and (iii) its convergence rate is smaller than a naive GD with a constant step size and asymptotically approaches to the lower bound of the first order method. These facts suggest that DUGD possibly accelerates the convergence speed by tuning step sizes properly.

¹If $n < T$, GD always converges to an optimal solution after n iterations by setting step sizes to the reciprocal of eigenvalues of \mathbf{A} . We thus omit this case.

A. Spectral radius and loss minimization

Training process of deep unfolding consists of minimizing a loss function. Here we show that minimizing a typical MSE loss also reduces the spectral radius $\rho(\mathbf{Q}^{(T)})$.

Before describing this claim, we first show the relation of $\rho(\mathbf{Q}^{(T)})$ to the eigenvalues of \mathbf{A} . Recall that the Hermitian positive definite matrix \mathbf{A} has n positive eigenvalues including degeneracy. Hereinafter, we assume that $\lambda_1 \neq \lambda_n$ to avoid a trivial case.

Lemma III.1. *Let $\{\lambda_i\}_{i=1}^n$ be an eigenvalue sequence of \mathbf{A} satisfying $(0 <) \lambda_1 \leq \lambda_2 \leq \dots \leq \lambda_n$. Then, we have*

$$\rho(\mathbf{Q}^{(T)}) = \max_{i=1,\dots,n} \left| \prod_{t=0}^{T-1} (1 - \gamma_t \lambda_i) \right|. \quad (7)$$

Proof. This is directly derived from (4) and the following fact: for a polynomial $p(x)$ with complex coefficients, if λ is an eigenvalue of \mathbf{A} associated with an eigenvector \mathbf{x} , then $p(\lambda)$ is an eigenvalue of the matrix $p(\mathbf{A})$ associated with the eigenvector \mathbf{x} [14, p. 4-11, 39]. \square

Using this lemma, we have the following theorem.

Theorem III.2. *Let $\mathbf{x}^{(0)} \in \mathbb{C}^n$ be a random variable over an isotropic p.d.f. $p(\mathbf{x}^{(0)})$ satisfying $0 < \mathbb{E}_{\mathbf{x}^{(0)}} \|\mathbf{x}^{(0)}\|_2^2 < \infty$. Then, for any $T \in \mathbb{N}$, there exists a positive constant C satisfying*

$$\rho(\mathbf{Q}^{(T)}) \leq C \sqrt{n \mathbb{E}_{\mathbf{x}^{(0)}} L(\mathbf{x}^{(T)})}. \quad (8)$$

The detail of the proof is found in Appendix B. This theorem claims that minimizing the MSE loss function in DUGD reduces the corresponding spectral radius of $\mathbf{Q}^{(T)}$ implying that a properly learned step size parameters can accelerate the convergence speed of DUGD.

B. Chebyshev step

In this subsection, our aim is to find a proper step size sequence that reduces the spectral radius to understand the nontrivial step size sequence of DUGD. When $T \geq 2$, minimizing $\rho(\mathbf{Q}^{(T)})$ with respect to $\{\gamma_t\}_{t=0}^{T-1}$ is a non-convex problem in general. In this subsection, we alternatively introduce a step size parameter sequence which bounds the spectral radius from above.

We first recall a well-known result when $T = 1$, i.e., a constant step-size case [2, Sec. 1.3].

Proposition III.3. *Let $\lambda_1(> 0)$ and λ_n be the minimum and maximum eigenvalues of \mathbf{A} , respectively. When $T = 1$, the step size parameter that minimizes $\rho(\mathbf{Q}^{(1)})$ is given by*

$$\gamma^* := \frac{2}{\lambda_1 + \lambda_n}. \quad (9)$$

In a general case in which $T \geq 2$, we focus on a step size sequence minimizing the upper bound $\rho^{\text{upp}}(\mathbf{Q}^{(T)})$ of the spectral radius $\rho(\mathbf{Q}^{(T)})$. The upper bound is given by

$$\begin{aligned} \rho(\mathbf{Q}^{(T)}) &= \max_{i=1,\dots,n} \left| \prod_{t=0}^{T-1} (1 - \gamma_t \lambda_i) \right| \\ &\leq \max_{\lambda \in [\lambda_1, \lambda_n]} \left| \prod_{t=0}^{T-1} (1 - \gamma_t \lambda) \right| := \rho^{\text{upp}}(\mathbf{Q}^{(T)}). \end{aligned} \quad (10)$$

Analyzing this upper bound is commonly used [24, Sec. 3.4].

Next, we introduce a step size parameter sequence called Chebyshev steps which minimizes the above upper bound.

Theorem III.4. *Let $\lambda_1(> 0)$ and λ_n be the minimum and maximum eigenvalues of \mathbf{A} , respectively. For a given $T \in \mathbb{N}$, we define Chebyshev steps $\{\gamma_t\}_{t=0}^{T-1}$ of length T by*

$$\gamma_t := \left[\frac{\lambda_n + \lambda_1}{2} + \frac{\lambda_n - \lambda_1}{2} \cos \left(\frac{2t+1}{2T} \pi \right) \right]^{-1}. \quad (11)$$

Then, it is a sequence that minimizes the upper bound $\rho^{\text{upp}}(\mathbf{Q}^{(T)})$ of spectral radius of $\mathbf{Q}^{(T)}$.

Note that the Chebyshev step is identical to an optimal constant step size in Prop. III.3 when $T = 1$.

Here, we describe a sketch of the proof. The complete version is available in Appendix C. The function $\prod_{t=0}^{T-1} (1 - \gamma_t \lambda)$ substituting Chebyshev steps is represented by a Chebyshev polynomial $C_T(x)$ of order T . Using the minimax property that $2^{1-T} C_T(x)$ is a monic polynomial that minimizes the ℓ_∞ -norm in the Banach space $B[-1, 1]$ [24, Col. 3.4B], we can prove that Chebyshev steps minimize $\rho^{\text{upp}}(\mathbf{Q}^{(T)})$.

The reciprocal of Chebyshev steps $z_t := \gamma_t^{-1}$ corresponds to Chebyshev points, i.e., zeros of a shifted Chebyshev polynomial of order T defined on $[\lambda_1, \lambda_n]$. Figure 3 shows Chebyshev points and Chebyshev steps when $T = 7$, $\lambda_1 = 1$, and $\lambda_n = 9$. A Chebyshev point is defined as a point projected onto an axis from a point of degree $\theta_t = (2t+1)\pi/(2T)$ on a semi-circle (see right part). Chebyshev points locate symmetrically with respect to the center of the circle corresponding to $(\gamma^*)^{-1} = (\lambda_1 + \lambda_n)/2$. Chebyshev steps are given by $\gamma_t = z_t^{-1}$, which is shown in the left part of Fig. 3. We find that the Chebyshev steps widely locate compared with the optimal constant step size $\gamma^* = 1/5$.

C. Convergence analysis

As a convergence analysis, we first show that GD with Chebyshev steps converges to the optimal solution. Let $\mathbf{Q}_{\text{Ch}}^{(T)}$ be a matrix $\mathbf{Q}^{(T)}$ substituting Chebyshev steps of length T .

Proposition III.5. *For any $k = 0, 1, 2, \dots$ and $T \in \mathbb{N}$, we have*

$$\|\mathbf{x}^{((k+1)T)} - \mathbf{x}_{\text{opt}}\|_2 \leq \rho^{\text{upp}}(\mathbf{Q}_{\text{Ch}}^{(T)}) \|\mathbf{x}^{(kT)} - \mathbf{x}_{\text{opt}}\|_2. \quad (12)$$

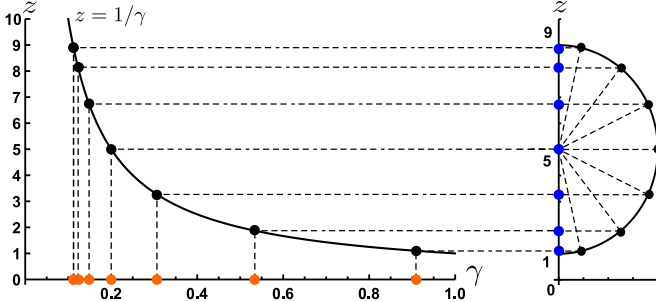


Fig. 2. Chebyshev points $\{z_t\}_{t=0}^{T-1}$ (right; blue) and corresponding Chebyshev steps $\{\gamma_t\}_{t=0}^{T-1}$ (left; orange) when $T = 7$, $\lambda_1 = 1$, and $\lambda_n = 9$.

Proof. Let $\|\mathbf{A}\|_{\text{op}} := \sup_{\|\mathbf{v}\|_2=1} \|\mathbf{A}\mathbf{v}\|_2$ be an operator norm of \mathbf{A} . Since $\mathbf{Q}_{\text{Ch}}^{(T)}$ is a normal matrix, $\|\mathbf{Q}_{\text{Ch}}^{(T)}\|_{\text{op}} = \rho(\mathbf{Q}_{\text{Ch}}^{(T)})$ holds. Using (5), (10), and $\mathbf{x}_{\text{opt}} = \mathbf{0}$, we have

$$\begin{aligned} \|\mathbf{x}^{((k+1)T)}\|_2 &= \|\mathbf{Q}_{\text{Ch}}^{(T)} \mathbf{x}^{(kT)}\|_2 \\ &\leq \|\mathbf{Q}_{\text{Ch}}^{(T)}\|_{\text{op}} \|\mathbf{x}^{(kT)}\|_2 \\ &= \rho(\mathbf{Q}_{\text{Ch}}^{(T)}) \|\mathbf{x}^{(kT)}\|_2 \\ &\leq \rho^{\text{upp}}(\mathbf{Q}_{\text{Ch}}^{(T)}) \|\mathbf{x}^{(kT)}\|_2. \end{aligned} \quad (13)$$

□

The main claim in this subsection is that Chebyshev steps of length $T (\geq 2)$ accelerate the convergence speed with respect to a spectral radius.

Theorem III.6. *Let \mathbf{Q}_{ch}^T be a matrix $\mathbf{Q}^{(T)}$ with Chebyshev steps of length $T (\geq 2)$. We also define \mathbf{Q}_{s}^T as $\mathbf{Q}^{(T)}$ with an optimal constant step size, i.e., $\gamma_0 = \dots = \gamma_{T-1} = \gamma^*$. Then, we have*

$$\rho(\mathbf{Q}_{\text{ch}}^{(T)}) < \rho(\mathbf{Q}_{\text{s}}^{(T)}). \quad (14)$$

The proof of this theorem is separated into two parts. First, using (10) and the definition of Chebyshev steps, we show that the spectral radius $\rho(\mathbf{Q}_{\text{ch}}^{(T)})$ is bounded by

$$\begin{aligned} \rho(\mathbf{Q}_{\text{ch}}^{(T)}) &\leq \rho^{\text{upp}}(\mathbf{Q}_{\text{Ch}}^{(T)}) \\ &= \left\{ \frac{1}{2} \left[\left(\frac{\sqrt{\kappa} + 1}{\sqrt{\kappa} - 1} \right)^T + \left(\frac{\sqrt{\kappa} - 1}{\sqrt{\kappa} + 1} \right)^T \right] \right\}^{-1}, \end{aligned} \quad (15)$$

where $\kappa := \lambda_n/\lambda_1$ is a condition number of the matrix \mathbf{A} . Second, we prove that $\rho^{\text{upp}}(\mathbf{Q}_{\text{Ch}}^{(T)}) < \rho(\mathbf{Q}_{\text{s}}^T) = [(\kappa - 1)/(\kappa + 1)]^T$. Further detail can be found in Appendix D.

The convergence rate of GD is defined by $R := \liminf_{t \rightarrow \infty} \rho(\mathbf{Q}^{(t)})^{1/t}$. In the constant step-size case, the convergence rate is $(\kappa - 1)/(\kappa + 1)$. From (15), the convergence rate $R_{\text{CHGD}}(T)$ of GD with Chebyshev steps (CHGD) of length T is bounded by

$$R_{\text{CHGD}}(T) \leq \left\{ \frac{1}{2} \left[\left(\frac{\sqrt{\kappa} + 1}{\sqrt{\kappa} - 1} \right)^T + \left(\frac{\sqrt{\kappa} - 1}{\sqrt{\kappa} + 1} \right)^T \right] \right\}^{-\frac{1}{T}}, \quad (16)$$

which is lower than the convergence rate of GD with an optimal constant step size $R_{\text{S}} = (\kappa - 1)/(\kappa + 1)$. The rate

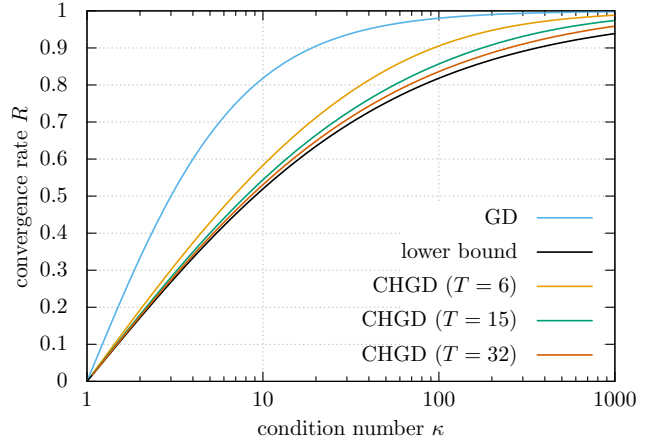


Fig. 3. Comparison of convergence rates as functions of condition number κ .

$R_{\text{CHGD}}(T)$ approaches to the well-known lower bound of first order methods from above, which is given by

$$R_{\text{low}} := \frac{\sqrt{\kappa} - 1}{\sqrt{\kappa} + 1}. \quad (17)$$

This bound is strict in that some GD algorithms such as the momentum method and Nesterov acceleration can achieve this rate in the strongly convex case. In Fig. 3, we show the convergence rates of GD and CHGD as functions of κ . For CHGD, some upper bounds of convergence rates with different T are plotted. It is confirmed that CHGD with $T \geq 2$ has a smaller convergence rate than GD with the optimal constant step size and the rate of CHGD approaches to the lower bound (16) quickly as T increases. All rates and the lower bound converge to 1 in the large- κ limit.

In summary, we focus on the fact that training process of DUGD reduces the spectral radius $\rho(\mathbf{Q}^{(T)})$ and introduce learning-free Chebyshev step that minimize its upper bound and improve the convergence rate.

IV. NUMERICAL COMPARISON TO DUGD

In this section, we examine DUGD following the setup in Sec II. The main goal is to examine whether Chebyshev steps explain the nontrivial learned step size parameters in DUGD. In addition, we also analyze the convergence property of DUGD and CHGD numerically.

A. Experiment conditions

We first describe the detail of numerical experiments. DUGD is implemented by PyTorch 1.3 [29]. Each training data is given by a pair of random initial point $\mathbf{x}^{(0)} \in \mathbb{R}^n$ and optimal solution $\mathbf{x}_{\text{opt}} = \mathbf{0}$. A random initial point is generated as an i.i.d. Gaussian random vector with unit mean and unit variance. A matrix \mathbf{A} is generated by $\mathbf{A} = \mathbf{H}^T \mathbf{H}$ with random Gaussian matrix $\mathbf{H} \in \mathbb{R}^{m \times n}$ whose elements are i.i.d. Gaussian random variables with zero mean and variance $1/n$. In this case, the eigenvalue distribution of \mathbf{A} follows the Marchenko-Pastur distribution as $n \rightarrow \infty$ with m/n fixed

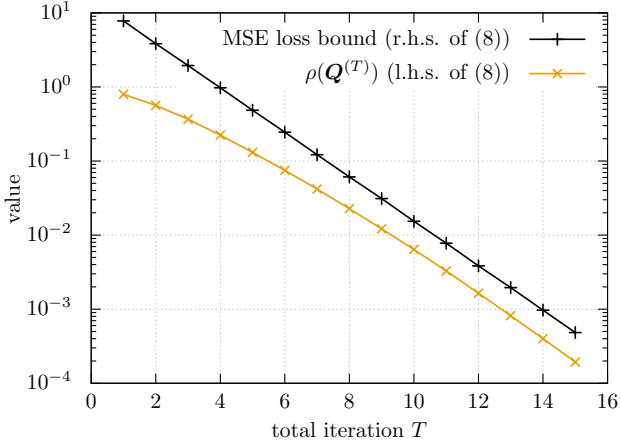


Fig. 4. Comparison of the MSE loss bound in Thm. III.2 and spectral radius $\rho(Q^{(T)})$ in DUGD when $(n, m) = (300, 1200)$.

to a constant. Then, the maximum and minimum eigenvalues approach to $(1 + \sqrt{m/n})^2$ and $(1 - \sqrt{m/n})^2$, respectively. Here we assume that the matrix \mathbf{A} is fixed throughout a whole process.

Its training process is executed by incremental training in which we gradually increase the number of layers (iterations T) by initializing the value of a parameter γ_t ($t = 0, \dots, T-1$) to a learned value in the former training process (generation) [15], [25]. Incremental training can improve the performance of DUGD compared with a conventional one-shot training in which all layers are trained at once. In the beginning of the whole training process, all initial values of $\{\gamma_t\}$ are set to 0.3. In each generation, parameters are optimized to minimize the MSE loss function $L(\mathbf{x}^{(T)})$ between an output of DUGD and the optimal solution using 500 mini-batch of size 200. We used Adam optimizer [19] of learning rate 0.002

B. Spectral radius and MSE loss

Here we numerically verify the relation between MSE loss in DUGD and the corresponding spectral radius $\rho(Q^{(T)})$ in Thm. III.2 up to $T = 15$. Figure 4 shows an example of the comparison when $n = 300$ and $m = 1200$. To estimate an average MSE loss $E_{\mathbf{x}^{(0)}} L(\mathbf{x}^{(T)})$, we use an empirical MSE loss after the T th generation. The constant C in the r.h.s. of (8) is evaluated numerically (see Appendix B). We confirm that the spectral radius $\rho(Q^{(T)})$ is upper bounded by (8) with the MSE loss $L(\mathbf{x}^{(T)})$.

C. Trained step sizes

Next we examine a learned step size parameter sequence in DUGD. Figure 5 shows examples of sequences of length $T = 6$ and 15 when $n = 300$ and $m = 1200$. To compare these parameters directly, they are rearranged in a descending order although learned parameters indeed show a zig-zag shape. The black symbols represent Chebyshev steps when we use asymptotic maximal eigenvalue $\lambda_n = 9$ and minimum eigenvalue $\lambda_1 = 1$ when $m/n = 4$. Other symbols show learned step size parameters corresponding to five trials, i.e.,

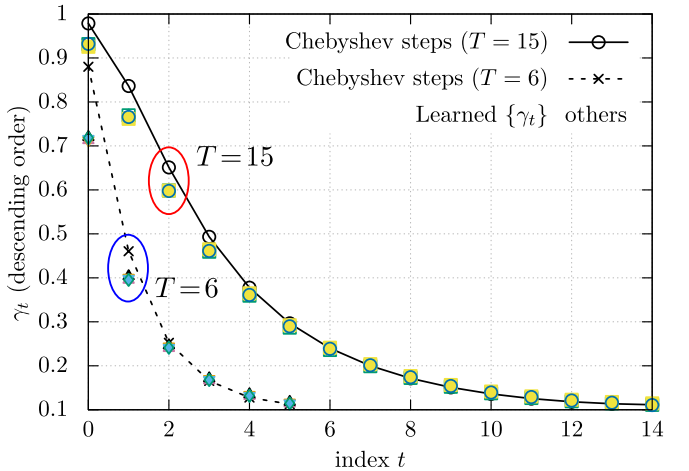


Fig. 5. Chebyshev steps (black symbols) and learned step size parameters in DUGD (others; 5 trials) in a descending order when $(n, m) = (300, 1200)$ and $T = 6$ (dotted) and 15 (solid).

different matrices of \mathbf{A} and training process with different random numbers. We find that the learned step sizes agree with each other indicating a self-average property of random matrices and success of training process. More importantly, they are close to Chebyshev steps especially when γ is small. It is also found that, when $T = 6$, the gap between Chebyshev steps and learned step sizes is larger than the $T = 15$ case.

The zig-zag shape of learned step size parameters is another nontrivial behavior of DUGD although the order of parameters does not affect the MSE performance after the T th iteration. It is numerically suggested that the shape depends on the training process, especially on the incremental training and initial values of $\{\gamma_t\}$. In fact, we can find a permutation of Chebyshev steps systematically by solving an optimization problem that emulates the training process. Figure 6 shows the learned step size parameters in DUGD ($T = 11$) with different initial values of $\{\gamma_t\}$ and corresponding permuted Chebyshev steps. We find that they agree with each other including the order of parameters. Further detail is available in Appendix E.

To understand the discrepancy between Chebyshev steps and learned step sizes, we show the absolute eigenvalues of $\mathbf{Q}^{(T)}$ as a function of eigenvalues of \mathbf{A} in Fig. 7. If the step size sequence of length T is given by $\{\gamma_t\}_{t=0}^{T-1}$, the absolute eigenvalues of $\mathbf{Q}^{(T)}$ corresponding to an eigenvalue λ of \mathbf{A} is written by $|\tau(\lambda)| = \left| \prod_{t=0}^{T-1} (1 - \gamma_t \lambda) \right|$. Figure 7 shows $|\tau(\lambda)|$ when $\{\gamma_t\}_{t=0}^{T-1}$ is a learned step size parameter sequence (red) and Chebyshev steps (black) of length $T = 6$. To show the spectral density, symbols are located at each eigenvalue λ_i of matrix \mathbf{A} . It is found that $\{|\tau(\lambda_i)|\}$ of learned step sizes are smaller than those of Chebyshev steps in the high spectral-density regime and larger otherwise. This is because it can reduces the MSE loss that all the eigenvalues of matrix \mathbf{A} contributes. In contrast, it increases the maximum value of $|\tau(\lambda_i)|$ corresponding to the spectral radius $\rho(Q^{(T)})$. In this case, the spectral radius of DUGD takes 0.074 while that of Chebyshev steps is 0.029. Recalling that the spectral

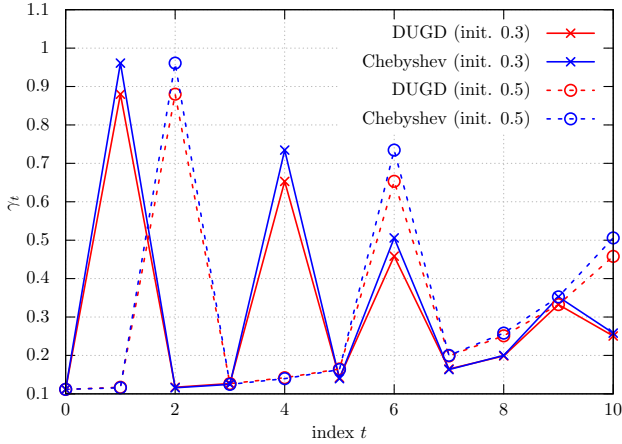


Fig. 6. Zig-zag shape of learned step size parameters (red) in DUGD and permuted Chebyshev steps (cross marks) with different initial values of γ when $(n, m) = (300, 1200)$ and $T = 11$.

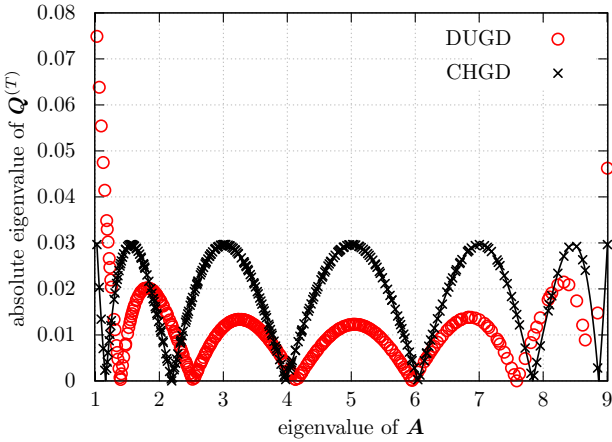


Fig. 7. Absolute eigenvalues of $\mathbf{Q}^{(T)}$ using learned step size parameters (red) as a function of eigenvalues of \mathbf{A} when $T = 7$, $\lambda_1 = 1.0$, and $\lambda_n = 9.0$. Black symbols represent the corresponding absolute eigenvalues when Chebyshev steps are used.

radius of an optimal constant step size $\gamma = 1/5$ takes $(1 - 1/5)^6 \simeq 0.262$, DUGD accelerates the convergence speed in terms of the spectral radius $\rho(\mathbf{Q}^{(T)})$ while Chebyshev steps further improves the convergence rate.

D. Performance analysis and convergence rate

Finally, we examine the convergence performance of DUGD and CHGD, and verify the convergence rate evaluated in Sec.III-C.

In the experiment, the MSE of DUGD is evaluated as a generalization error. In DUGD, we first train step sizes with $T = 15$ and repeat it for every 15 iterations. Similarly, CHGD are executed repeatedly with Chebyshev steps of length 15.

Figure 8 shows the MSE performance of DUGD, CHGD, and GD with the optimal constant step size when $(n, m) = (300, 1200)$. We find that DUGD and CHGD converge faster than GD, which shows that a proper step size parameter sequence in unfolded GD accelerates the convergence speed.

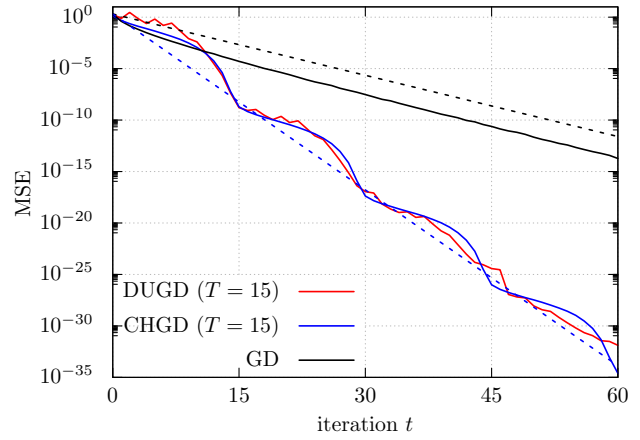


Fig. 8. Comparison of MSE performance of GD algorithms when $(n, m) = (300, 1200)$ ($\kappa = 8.79$). Dotted lines represent slopes of the convergence rate of CHGD (16) and GD R_S .

Although DUGD shows slightly better MSE performance than CHGD when $t = 15$, CHGD exhibits faster convergence as the number of iterations increases. This is because the spectral radius of CHGD is smaller than that of DUGD as discussed in the last subsection. Figure 8 also shows the MSE calculated by (12) using the convergence rates. It is found that the upper bound of convergence rate (16) correctly predicts the convergence property of CHGD.

In summary, we numerically verify theoretical analyses in the last section, and find that Chebyshev steps qualitatively reproduces a learned step size sequence in DUGD. It also indicates that deep unfolding can accelerate the GD algorithm by tuning its step size parameters.

V. APPLICATION OF CHEBYSHEV STEPS

In this section, we consider an application of CHGD instead of DUGD because CHGD requires no training process. After we compare CHGD with other accelerated GD algorithms, we demonstrate a practical application of CHGD to ridge regression.

A. Comparison to accelerated GD

Here, we compare CHGD with two GD algorithms with a momentum term. One is the momentum method (MOM) whose recursive relation is given by

$$\mathbf{x}^{(t+1)} = (\mathbf{I}_n - \gamma' \mathbf{A}) \mathbf{x}^{(t)} + \beta (\mathbf{x}^{(t)} - \mathbf{x}^{(t-1)}), \quad (18)$$

where $\mathbf{x}^{(-1)} = \mathbf{0}$, $\gamma' := 4/(\sqrt{\lambda_1} + \sqrt{\lambda_n})^2$ and $\beta := ((\sqrt{\kappa} - 1)/(\sqrt{\kappa} + 1))^2$ [30]. The other is the Chebyshev semi-iterative method (CH-semi) defined as

$$\begin{aligned} \mathbf{x}^{(t+1)} &= (\mathbf{I}_n - \gamma'_{t+1} \mathbf{A}) \mathbf{x}^{(t)} + (\gamma'_{t+1} - 1) (\mathbf{x}^{(t)} - \mathbf{x}^{(t-1)}), \\ \gamma'_{t+1} &= \frac{4}{4 - \xi^2 \gamma'_t} \quad (t \geq 2), \end{aligned} \quad (19)$$

where $\mathbf{x}^{(-1)} = \mathbf{0}$, $\gamma'_1 = 1$, $\gamma'_2 = 2/(2 - \xi^2)$, and $\xi = 1 - 1/\kappa$ [9]. These achieve the lower bound (17) of convergence rate.

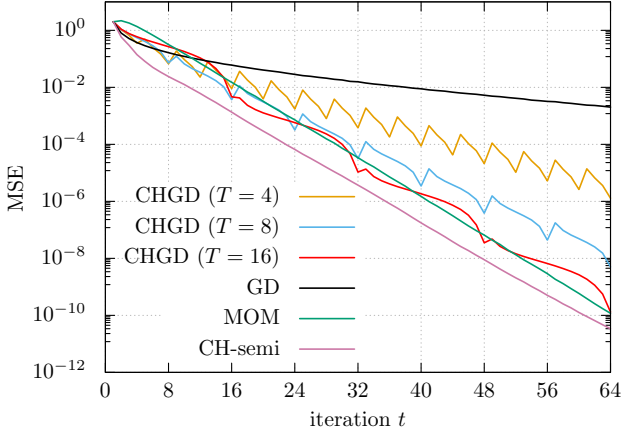


Fig. 9. MSE performance of CHGD with $T = 4, 8, 16$ and other GD algorithms when $(n, m) = (300, 600)$ ($\kappa = 88.1$).

Figure 9 shows the MSE performance of CHGD with $T = 4, 8, 16$ and other GD algorithms. It is found that CHGD gradually improve its MSE performance as T increases. In particular, CHGD ($T = 16$) has reasonable performance compared with MOM and CH-semi. It indicates that CHGD is an *accelerated GD algorithm without momentum terms*.

B. Applications to ridge regression for real data

Here, we demonstrate CHGD for ridge regression. Ridge regression, also known as Tikhonov regularization, is a fundamental biased estimation for ill-conditioned problems [13]. Let us consider a noisy linear observation $\mathbf{y} = \mathbf{H}\beta + \mathbf{n}$ with a measurement matrix $\mathbf{H} \in \mathbb{R}^{m \times n}$. When $m \gg n$, the LMS problem becomes ill-conditioned leading to numerical instability. Instead, the ridge regression is often used, which is defined by

$$\hat{\beta} := \operatorname{argmin}_{\beta \in \mathbb{R}^n} \frac{1}{2} \|\mathbf{y} - \mathbf{H}\beta\|_2^2 + \frac{\eta}{2} \|\beta\|_2^2, \quad (20)$$

where η is a regularization coefficient controlling weights of the estimate $\hat{\beta}$. As the parameter η reduces the condition number of the matrix $\mathbf{H}^T \mathbf{H} + \eta \mathbf{I}_n$, a simple ridge estimator $(\mathbf{H}^T \mathbf{H} + \eta \mathbf{I}_n)^{-1} \mathbf{H}^T \mathbf{y}$ is available. However, it takes $O(n^3)$ computation time to calculate a pseudo-inverse matrix. This computational cost becomes more costly if one searches a proper η by sweeping its value.

An alternative way to solve (20) is the use of GD algorithms. Since it contains no inverse of a matrix, it runs in $O(n^2)$ time. The drawback of GD is its slow convergence when η is relatively small. In this sense, using a GD algorithm with faster convergence is important.

To examine the convergence speed of GD algorithm in ridge regression, we examine the three algorithms; GD with an optimal constant step size, CHGD, and momentum method (19). As an example, ridge regression is applied to Communities and Crime Data Set [31] in UCI Machine Learning Repository [6]. After removing elements containing missing values, the dimensions of β and \mathbf{y} are $n = 98$ and $m = 1994$,

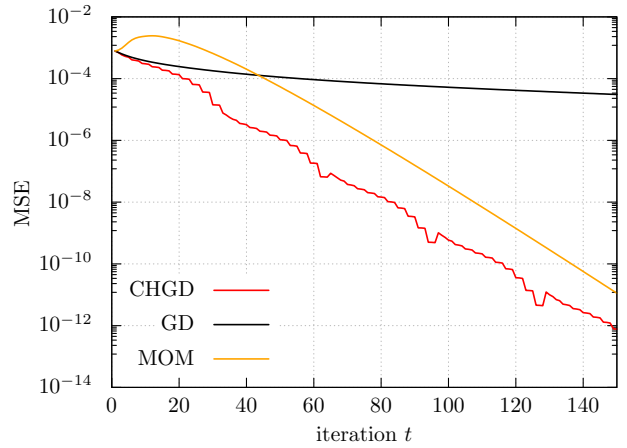


Fig. 10. Convergence performance of GD algorithm in Ridge regression ($\eta = 158.48$) of crime data. In CHGD, T is set to 32.

respectively. The moment matrix $\mathbf{A} = \mathbf{H}^T \mathbf{H}$ has a huge condition number $\kappa \simeq 7.8 \times 10^5$ indicating the inverse problem is ill-conditioned. In the experiments, all algorithms use the maximum and minimum values of the matrix \mathbf{A} . By using the power method, we can estimate the maximum eigenvalue λ_n in $O(n^2)$ time instead of computing eigenvalues directly in $O(n^3)$ time. For the estimation of the minimum eigenvalue, the power method is also applicable to a shifted matrix $\lambda_n \mathbf{I}_n - \mathbf{A}$ because \mathbf{A} is positive definite.

Figure 10 shows the MSE performance between the ridge estimation and estimates of GD algorithms as a function of the iteration index t when $\eta = 158.48$. In CHGD, we set $T = 32$ and the order of Chebyshev steps is properly permuted (see Appendix F). It is found that the momentum method takes some iteration steps to exhibit better MSE performance than GD although its convergence speed is much faster for large t . Although the MSE of CHGD forms a wavy shape, estimates at every $T = 32$ steps are reasonably accurate and converges quickly. We thus find that CHGD exhibits fast convergence compared with the other algorithms. In addition, CHGD requires no momentum terms and thus less computational resources, which would be advantageous for extremely large data set.

VI. CONCLUDING REMARKS

In this paper, we study a nontrivial learned step size sequence appeared in DUGD. We prove that minimizing the MSE loss in DUGD reduces the spectral radius related to the convergence rate. In addition, we introduce learning-free Chebyshev steps that minimizes the the upper bound of the spectral radius. It is shown that Chebyshev steps accelerate the convergence speed compared with a naive GD and the rate approaches to the strict lower bound of the first order method in a specific limit. Numerical results support the analyses and shows that Chebyshev steps reproduces the learned step size sequence in DUGD, which provides a plausible interpretation of the learned parameters. Moreover, CHGD exhibits reason-

able convergence speed compared with other accelerated GD algorithms although it does not require a momentum term.

There are several open problems. One direction is the extension of the analysis in this paper to convex and non-convex problems other than quadratic convex problems. Another direction is an application of Chebyshev steps to other GD-based algorithms such as stochastic gradient descent.

ACKNOWLEDGEMENT

This work was partly supported by JSPS Grant-in-Aid for Scientific Research (B) Grant Number 19H02138 (TW), JSPS Grant-in-Aid for Early-Career Scientists Grant Number 19K14613 (ST), and the Telecommunications Advancement Foundation (ST).

APPENDIX A EXPERIMENTAL SETTING OF FIGURE 1

Here, we describe experimental setting of Fig. 1 in the main text.

We consider noiseless measurement $\mathbf{y} = \mathbf{H}\beta$ where a measurement matrix $\mathbf{H} \in \mathbb{R}^{m \times n}$ is a Gaussian random matrix whose elements are i.i.d. Gaussian random variables with zero mean and variance $1/n$. We assume that $(n, m) = (300, 600)$ and each element of β follows the normal distribution. DUGD is defined by

$$\beta^{(t+1)} = \beta^{(t)} - \gamma_t \mathbf{H}^T (\mathbf{y} - \mathbf{H}\beta^{(t)}) \quad (t = 0, \dots, T-1), \quad (21)$$

where T is the total number of iterations (or layers) and $\{\gamma_t\}$ are trainable step size parameters. The initial estimate is given by $\beta^{(0)} = \mathbf{0}$.

DUGD is implemented by PyTorch 1.3 [29]. Each training data is given by a pair of a true solution β and the corresponding measurement vector $\tilde{\mathbf{y}}$ for a given \mathbf{H} . Its training process is executed by incremental training in which we gradually increase the number of layers (iterations T) by initializing the value of parameters $\{\gamma_t\}$ ($t = 0, \dots, T-1$) according to learned values in the former training process (generation) to improve the performance of DUGD. In the beginning of the whole training process, all initial values of $\{\gamma_t\}$ are set to 0.3. In each generation, the parameters are optimized by Adam optimizer [19] of learning rate 0.002 to minimize the MSE loss function $\|\tilde{\beta} - \beta^{(T)}\|_2^2/n$ between an output of DUGD using $\tilde{\mathbf{y}}$ and the true solution $\tilde{\beta}$. As a mini-batch training, 500 mini-batches of size 200 are used in each generation. The MSE is measured as

APPENDIX B PROOF OF THEOREM 3.2

Proof. As the matrix \mathbf{A} is an Hermitian matrix, it can be decomposed by $\mathbf{A} = \mathbf{U}\Lambda\mathbf{U}^*$ using an unitary matrix \mathbf{U}

and diagonal matrix $\Lambda := \text{diag}(\lambda_1, \dots, \lambda_n)$ with eigenvalues $\lambda_1, \dots, \lambda_n$ of \mathbf{A} . Then, we have

$$\begin{aligned} \mathbb{E}_{\mathbf{x}^{(0)}} L(\mathbf{x}^{(T)}) &= \frac{1}{n} \mathbb{E}_{\mathbf{x}^{(0)}} \left\| \prod_{t=0}^{T-1} (\mathbf{I}_n - \gamma_t \mathbf{U} \Lambda \mathbf{U}^*) \mathbf{x}^{(0)} \right\|_2^2 \\ &= \frac{1}{n} \mathbb{E}_{\mathbf{x}^{(0)}} \left\| \mathbf{U} \left(\prod_{t=0}^{T-1} (\mathbf{I}_n - \gamma_t \Lambda) \right) \mathbf{U}^* \mathbf{x}^{(0)} \right\|_2^2 \\ &= \frac{1}{n} \mathbb{E}_{\mathbf{x}^{(0)}} \left\| \left(\prod_{t=0}^{T-1} (\mathbf{I}_n - \gamma_t \Lambda) \right) \mathbf{U}^* \mathbf{x}^{(0)} \right\|_2^2 \\ &:= \frac{1}{n} \mathbb{E}_{\mathbf{x}^{(0)}} \left\| \mathbf{D}^{(T)} \mathbf{U}^* \mathbf{x}^{(0)} \right\|_2^2 \end{aligned} \quad (22)$$

where $\mathbf{D} := \text{diag}(\prod_{t=0}^{T-1} (1 - \gamma_t \lambda_i))$ is the diagonal matrix whose (i, i) -element is an eigenvalue of $\mathbf{Q}^{(T)}$ corresponding to the eigenvalue λ_i of \mathbf{A} . In the last line, we use $\mathbf{U}\mathbf{U}^* = \mathbf{I}_n$. Introducing column vectors of \mathbf{U} by $\mathbf{U} := (\mathbf{u}_1, \dots, \mathbf{u}_n)$, $\mathbf{U}^* \mathbf{x}_0 = (\mathbf{u}_1^* \mathbf{x}_0, \dots, \mathbf{u}_n^* \mathbf{x}_0)^T$ holds.

Using $j := \text{argmax}_i |\prod_{t=0}^{T-1} (1 - \gamma_t \lambda_i)|$, we have

$$\begin{aligned} L(\mathbf{x}^{(T)}) &= \frac{1}{n} \mathbb{E}_{\mathbf{x}^{(0)}} \left\| \sum_{i=1}^n \mathbf{D}_{i,i}^{(T)} \mathbf{u}_i^* \mathbf{x}^{(0)} \right\|_2^2 \\ &\geq \frac{1}{n} \left| \prod_{t=0}^{T-1} (1 - \gamma_t \lambda_j) \right|^2 \mathbb{E}_{\mathbf{x}^{(0)}} \left\| \mathbf{u}_j^* \mathbf{x}^{(0)} \right\|_2^2 \\ &:= \frac{C'}{n} \left| \prod_{t=0}^{T-1} (1 - \gamma_t \lambda_j) \right|^2, \end{aligned} \quad (23)$$

where $C' := \mathbb{E}_{\mathbf{x}^{(0)}} \|\mathbf{u}_j^* \mathbf{x}^{(0)}\|^2 (< \infty)$ is a positive constant because the p.d.f. of $\mathbf{x}^{(0)}$ is homogeneous. Recalling that $\rho(\mathbf{Q}^{(T)}) = \max_i |\prod_{t=0}^{T-1} (1 - \gamma_t \lambda_i)| = |\prod_{t=0}^{T-1} (1 - \gamma_t \lambda_j)|$ from Lemma 3.1, we have $\mathbb{E}_{\mathbf{x}^{(0)}} L(\mathbf{x}^{(T)}) \geq C' \rho(\mathbf{Q}^{(T)})^2/n$, which is identical to (8). \square

The proof indicates that the constant C is explicitly given by $C = (\mathbb{E}_{\mathbf{x}^{(0)}} \|\mathbf{u}_j^* \mathbf{x}^{(0)}\|^2)^{-1/2}$ with $j := \text{argmax}_i |\prod_{t=0}^{T-1} (1 - \gamma_t \lambda_i)|$. In the special case where each element of $\mathbf{x}^{(0)}$ is an i.i.d. random variable, C can be easily calculated. This fact is used in the numerical experiment in Sec. 4.1.

APPENDIX C PROOF OF THEOREM 3.4

Before we will give a proof of Thm. 3.4, we prove the following lemma related to the minimax property of Chebyshev polynomials. The Chebyshev polynomial $C_n(x)$ of degree n ($n = 0, 1, \dots$) is defined by a recursive relation $C_{n+1}(x) := 2x C_n(x) - C_{n-1}(x)$ with $C_0(x) := 1$ and $C_1(x) := x$. Let $C[a, b]$ ($a < b$) be the Banach space defined by ℓ_∞ -norm, i.e., $\|f\| := \max_{x \in [a, b]} |f(x)|$.

Lemma C.1. *Suppose that $b > a > 0$. Let $D \subset C[a, b]$ be a subspace of polynomials of z on $[a, b]$ represented by*

$\prod_{k=0}^{n-1} (1 - \alpha_k z)$ for any $\alpha_0, \dots, \alpha_{n-1} \in \mathbb{R}$. We define the Chebyshev steps of length n by

$$\gamma_k := \left[\frac{a+b}{2} + \frac{b-a}{2} \cos \left(\frac{2k+1}{2n} \pi \right) \right]^{-1} \quad (k = 0, 1, \dots, n-1), \quad (24)$$

and a normalized Chebyshev polynomial $\hat{\varphi}(z)$ of degree n by

$$\hat{\varphi}(z) := \frac{C_n \left(\frac{2z-a-b}{b-a} \right)}{C_n \left(-\frac{a+b}{b-a} \right)}. \quad (25)$$

Then, the following statements hold.

(a) The function $\hat{\varphi} : [a, b] \rightarrow \mathbb{R}$ belongs to D by setting $\alpha_k = \gamma_k^{-1}$ ($k = 0, 1, \dots, n-1$).

(b) The function $\hat{\varphi} : [a, b] \rightarrow \mathbb{R}$ is a polynomial in D that minimizes the norm $\|\cdot\|$.

Proof. (a) The Chebyshev polynomial $C_n(x)$ of degree n has n zeros in $(-1, 1)$, which are given by $x_k = \cos((2k+1)\pi/(2n))$ ($k = 0, \dots, n-1$) [24, Sec. 2.2]. Namely, $C_n(x) = \prod_{k=0}^{n-1} (x - x_k)$ holds. Then, using the affine transformation from $[a, b]$ to $[-1, 1]$, we have

$$C_n \left(\frac{2z-a-b}{b-a} \right) = \prod_{k=0}^{n-1} \left(z - \frac{1}{\gamma_k} \right). \quad (26)$$

Since $C_n(-(a+b)/(b-a)) = \prod_{k=0}^{n-1} (-\gamma_k^{-1})$, we have $\hat{\varphi}(z) = \prod_{k=0}^{n-1} (1 - \gamma_k z)$, which indicates that the statement holds.

(b) We will show that $\hat{\varphi}(z)$ is a minimizer of $\|\cdot\|$ among functions in D by indirect proof. Assume that there exists $\tau(z) \in D$ of at most degree n except for $\hat{\varphi}(x)$ satisfying $\|\hat{\varphi}(z)\| > \|\tau(z)\|$. As $\check{x}_k := \cos(k\pi/n)$ ($k = 0, \dots, n$) are the extreme points on $[-1, 1]$ (including both edge points) of $C_n(x)$ [24, Sec. 2.2], $\check{z}_k := (a+b)/2 + (b-a)\check{x}_k/2$ ($\in [a, b]$) are those of $\hat{\varphi}(z)$. Namely, the sign of the extremal value at \check{x}_k (or \check{z}_k) changes alternatively, i.e., $C_n(\check{x}_n) = 1$, $C_n(\check{x}_{n-1}) = -1$, $C_n(\check{x}_{n-2}) = 1$, and so on (or $\hat{\varphi}(\check{z}_n) = \varphi_0$, $\hat{\varphi}(\check{z}_{n-1}) = -\varphi_0$, $\hat{\varphi}(\check{z}_{n-2}) = \varphi_0$, and so on; $\varphi_0 := 1/C_n(-(a+b)/(b-a))$) hold [24, Lem. 3.6]. From the assumption, it indicates that $n+1$ inequalities, $\tau(\check{z}_n) < \varphi_0$, $\tau(\check{z}_{n-1}) > -\varphi_0$, $\tau(\check{z}_{n-2}) < \varphi_0$, and so on hold. In other words, a polynomial $\delta(z) := \tau(z) - \hat{\varphi}(z)$ of degree at most n has n zeros in $[a, b]$.

However, since $\tau(z), \hat{\varphi}(z) \in D$, the constant term of $\delta(z)$ is equal to zero suggesting that it has at most $n-1$ zeros in $[a, b]$. This results in contradiction by the assumption and shows that $\hat{\varphi} : [a, b] \rightarrow \mathbb{R}$ minimizes the norm $\|\cdot\|$ in D . \square

It is straightforward to show Thm. 3.4 from this lemma.

proof of Thm.3.4. Using the notation of Lemma C.1, we notice that $a = \lambda_1$, $b = \lambda_n$, and

$$\rho^{\text{upp}}(\mathbf{Q}^{(T)}) = \max_{\lambda \in [\lambda_1, \lambda_n]} \left| \prod_{t=0}^{T-1} (1 - \gamma_t \lambda) \right| = \left\| \prod_{t=0}^{T-1} (1 - \gamma_t \lambda) \right\|. \quad (27)$$

From Lemma C.1, the Chebyshev steps of length T is a sequence that minimizes $\rho^{\text{upp}}(\mathbf{Q}^{(T)})$. \square

APPENDIX D PROOF OF THEOREM 3.6

Proof. To simplify notations, we use $\kappa := \lambda_n/\lambda_1 (> 1)$ as a condition number of the matrix \mathbf{A} . From (10) and Lem. C.1, we have

$$\begin{aligned} \rho(\mathbf{Q}_{\text{Ch}}^{(T)}) &\leq \rho^{\text{upp}}(\mathbf{Q}_{\text{Ch}}^{(T)}) \\ &= \max_{x \in [\lambda_1, \lambda_n]} \hat{\varphi}(x) \\ &= \left| C_T \left(-\frac{\kappa+1}{\kappa-1} \right) \right|^{-1} \\ &= \left| (-1)^T \frac{(\sqrt{\kappa}+1)^{2T} + (\sqrt{\kappa}-1)^{2T}}{2(\kappa-1)^T} \right|^{-1} \\ &= \left\{ \frac{1}{2} \left[\left(\frac{\sqrt{\kappa}+1}{\sqrt{\kappa}-1} \right)^T + \left(\frac{\sqrt{\kappa}-1}{\sqrt{\kappa}+1} \right)^T \right] \right\}^{-1}. \end{aligned} \quad (28)$$

Here, we use properties that $|C_n(x)| \leq 1$ holds for $\forall x \in [-1, 1]$ and $C_n(x) = [(x+\sqrt{x^2-1})^n + (x-\sqrt{x^2-1})^n]/2$ for $|x| > 1$ hold, and an identity $x \pm \sqrt{x^2-1} = (\sqrt{\kappa} \pm 1)^2/(\kappa-1)$ when $x = (\kappa+1)/(\kappa-1)$.

On the other hand, the spectral radius when the optimal constant step size $\gamma_t^* = 2/(\lambda_1 + \lambda_n)$ is used can be calculated directly. We have

$$\rho(\mathbf{Q}_{\text{s}}^{(T)}) = \prod_{t=0}^{T-1} \max_i |1 - \gamma^* \lambda_i| = \left(\frac{\kappa-1}{\kappa+1} \right)^T. \quad (29)$$

Finally, we will show that $\rho^{\text{upp}}(\mathbf{Q}_{\text{Ch}}^{(T)}) < \rho(\mathbf{Q}_{\text{s}}^{(T)})$ holds. This is equivalent to the following relation for $\kappa > 1$.

$$\begin{aligned} &\frac{1}{2} \left[\left(\frac{\sqrt{\kappa}+1}{\sqrt{\kappa}-1} \right)^T + \left(\frac{\sqrt{\kappa}-1}{\sqrt{\kappa}+1} \right)^T \right] - \left(\frac{\kappa+1}{\kappa-1} \right)^T \\ &= \frac{(\sqrt{\kappa}+1)^{2T} + (\sqrt{\kappa}-1)^{2T} - 2(\kappa+1)^T}{2(\kappa-1)^T} > 0. \end{aligned} \quad (30)$$

If we set $X := \sqrt{\kappa} (> 1)$, the $(2t)$ th coefficient of $(X+1)^{2T}/2 + (X-1)^{2T}/2 - (X^2+1)^T$ is given by $\binom{2T}{2t} - \binom{T}{t}$. In addition, its coefficients of odd orders are equal to zero. From the Vandermonde's identity:

$$\binom{m+n}{r} = \sum_{k=0}^r \binom{m}{k} \binom{n}{r-k}, \quad (31)$$

we find

$$\binom{2T}{2t} = \sum_{l=0}^{2t} \binom{T}{l} \binom{T}{2t-l} \geq \binom{T}{t}^2 \geq \binom{T}{t}, \quad (32)$$

(equality holds only when $t = 0, T$), which indicates that (30) holds.

We thus show $\rho(\mathbf{Q}_{\text{Ch}}^{(T)}) \leq \rho^{\text{upp}}(\mathbf{Q}_{\text{Ch}}^{(T)}) < \rho(\mathbf{Q}_{\text{s}}^{(T)})$ when $\lambda_1 < \lambda_n$. \square

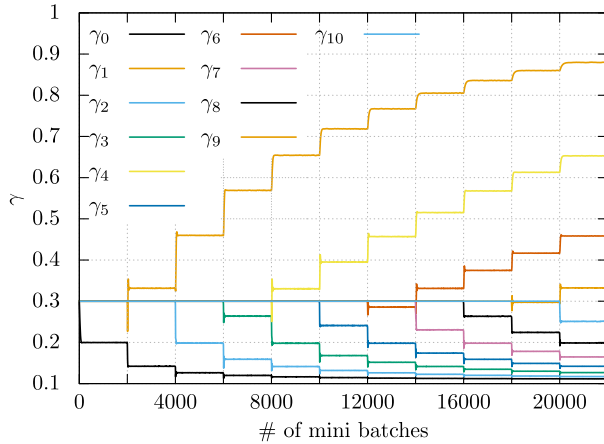


Fig. 11. Dynamics of step size parameters $\{\gamma_t\}_{t=0}^{10}$ of DUGD when $(n, m) = (300, 1200)$. Horizontal line represents the number of mini batches in incremental training. All initial values are set to 0.3. In incremental training, the number of learning parameter increases one by one every when 2000 mini batches are fed to DUGD. For example, only γ_0 (black) is trained during the first 2000 mini batches and γ_0 and γ_1 (orange) are trained during the next 2000 mini batches.

APPENDIX E ORDER OF LEARNED STEP SIZES

In this subsection, we describe how to find a permutation of Chebyshev steps that reproduces a zig-zag pattern of learned step size parameters of DUGD. A key observation is the dynamics of trainable step sizes parameters in training process.

Figure 11 shows the dynamics of trainable step size parameters. During incremental training, the number of trainable parameters increases at every 2000 mini batches. In other words, DUGD of T iterations (or layers) is trained from the 2000($T - 1$)th mini batches to the 2000 T th mini batches, which we call the T th generation of incremental training. After the T th generation ends, we add an initialized parameter γ_{T+1} to learned parameters $\{\gamma_t\}_{t=0}^T$ to start a new generation. As we can see Fig. 11, trainable parameters immediately move toward a (sub)optimal point to reduce the MSE loss function, which forms a staircase shape of γ_t . Although there are $T!$ optimal points of step sizes by permutation symmetry, it is numerically suggested that DUGD chooses an optimal point so that the “distance” (discussed later) from the former learned parameters is minimized. It seems natural because these parameters are updated by a GD-based optimizer and the convergent point depends on the initial point.

From these observations, we attempt to emulate the order of learned step size parameters using the Chebyshev steps. Let us consider a training process of DUGD minimizing the spectral radius $\rho(\mathbf{Q}^{(T)})$ instead of the MSE loss function. Although it seems practically difficult, we assume that we obtain the Chebyshev steps as an approximate solution. Here, the problem is which order of Chebyshev steps is chosen at every generations. We thus find an order of Chebyshev steps that minimizes a “distance” from a given initial point to a point whose elements are permuted Chebyshev steps. As a measure

Algorithm 1 Emulation of incremental training by Chebyshev steps

```

Input: maximum eigenvalue  $\lambda_1$ , minimum eigenvalue  $\lambda_n$ , number of iterations  $T$ , initial value  $u$ 
Initialize  $\mathbf{c} = (2/(\lambda_1 + \lambda_n))$ 
for  $t = 2$  to  $T$  do
  Set  $v$  to a sufficiently large number
   $\mathbf{d} = (\mathbf{c}, u)$ 
  Define  $\mathbf{c}$  as Chebyshev steps of length  $t$  for  $\lambda_1$  and  $\lambda_n$ 
  for  $\pi$  to all possible permutations  $\Pi(t)$  do
    Define  $\mathbf{P}_\pi$  as the permutation matrix of  $\pi$ 
    if  $v > \|\mathbf{d} - \mathbf{P}_\pi \mathbf{c}\|_2$  then
       $v = \|\mathbf{d} - \mathbf{P}_\pi \mathbf{c}\|_2$ ,  $\mathbf{P} = \mathbf{P}_\pi$ 
    end if
  end for
   $\mathbf{c} = \mathbf{P} \mathbf{c}$ 
end for
Return:  $\mathbf{c}$ 

```

of distance, we use a simple Euclidean norm because an actual distance defined by an energy landscape is difficult to be calculated. The detail of the algorithm is shown in Alg. 1. To emulate incremental training, the length of Chebyshev steps is gradually increased. As an initial point $(\gamma_1, \dots, \gamma_{t+1})$ of length $t+1$, $\gamma_1, \dots, \gamma_t$ are set to an optimally permuted Chebyshev steps in the last generation and γ_{t+1} is set to a given initial value. Then, an optimal permutation of the Chebyshev steps of length $t+1$ is searched so that its distance from the initial point takes the minimum value. The point is used as an initial point of the next generations. As shown in Fig. 6, it successfully reproduces the zig-zag shape of learned step size parameters that depends on an initial value of γ_t .

APPENDIX F ORDER OPTIMIZATION OF CHEBYSHEV STEPS

The order of Chebyshev steps is important practically to ensure numerical stability. Figure 12 shows the MSE performance of CHGD with different order of Chebyshev steps. It is found that the use of ascending order will lead to a search point with huge values that will cause a digit loss in this case. To avoid this instability, we need to permute the step size parameter sequence. It is noted that the performance of CHGD itself is ensured at every T iterations if numerical errors are ignorant. Since the total number of permutations rapidly diverges depending on T , we here focus on permutations defined by

$$\pi(t+1) \equiv a\pi(t) + b \pmod{T}, \quad (33)$$

where $\pi(0) := c \in \{0, 1, \dots, T-1\}$ is an initial index. It is known that the sequence $\{\pi(t)\}_{t=0}^{T-1}$ is a permutation of $\{0, 1, \dots, T-1\}$ if b is odd, $a \equiv 1 \pmod{4}$, and $T = 2^s$ ($s \in \mathbb{N}$). We then search parameters a, b, c satisfying this condition

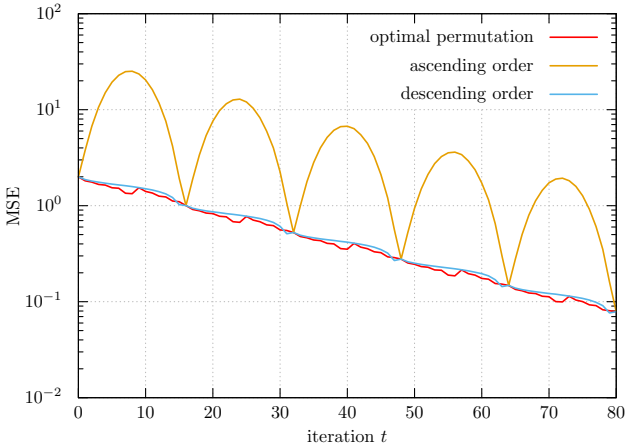


Fig. 12. MSE performance of CHGD ($T = 16$) with optimal permutation (red), ascending order (orange), and descending order (blue) when $(n, m) = (500, 800)$.

Algorithm 2 Permutation search

Input: maximum eigenvalue λ_n , minimum eigenvalue λ_1 , number of iterations $T := 2^s$ ($s \in \mathbb{N}$)
Set v to a sufficiently large number
Define c as the Chebyshev steps of length T for λ_1 and λ_n .
for (a, b, c) satisfying $1 \leq a, b, c \leq T - 1$, $a \equiv 1 \pmod{4}$, and b : odd **do**
 Define P as the permutation matrix corresponding to (a, b, c)
 if $v > \rho_{\text{temp}}(T)$ **then**
 $v = \rho_{\text{temp}}(T)$, $Q = P$
 end if
end for
Return: Pc , (a, b, c)

and minimizing a maximum temporal spectral radius of $\mathbf{W}^{(t)}$, i.e.,

$$\rho_{\text{temp}}(T) := \max_{t \in \{0, 1, \dots, T-1\}} \left(\max_{\lambda \in [\lambda_1, \lambda_n]} \left| \prod_{t'=0}^t (1 - \gamma_{t'} \lambda) \right| \right). \quad (34)$$

Algorithm 2 shows a pseudocode of the searching algorithm.

Figure 12 shows the MSE performance of CHGD ($T = 16$) with and without permutation when $n = 500$ and $m = 800$. In this case, the asymptotic value of the condition number is $\kappa = 8.54$ and optimal parameters are given by $(a, b, c) = (1, 9, 7)$. In CHGD without permutation, the step sizes is given by (24) in a descending or ascending way. Particularly, GD with ascending Chebyshev steps shows a relatively large MSE. Numerical results show that CHGD with optimal permutation decreases MSE effectively.

An example of (a, b, c) for different T , $\lambda_1 = 1$, and $\lambda_n = \kappa$ is given in Tab. I. It is found that the optimal choice of (a, b, c) depends on λ_1 and λ_n . In Sec. 5.2, the Chebyshev steps is permuted according to $(a, b, c) = (1, 11, 10)$.

TABLE I
PERMUTATION (a, b, c) OF CHEBYSHEV STEPS WHEN $\lambda_1 = 1$ AND $\lambda_n = \kappa$.

	$T = 8$	$T = 16$	$T = 32$
$\kappa = 4$	(1, 5, 3)	(1, 9, 7)	(1, 17, 15)
$\kappa = 16$	(1, 5, 3)	(1, 9, 7)	(1, 17, 15)
$\kappa = 64$	(1, 3, 2)	(1, 9, 7)	(1, 17, 15)
$\kappa = 128$	(1, 3, 2)	(13, 3, 6)	(1, 17, 15)

REFERENCES

- P. Ablin, T. Moreau, M. Massias, and A. Gramfort. Learning step sizes for unfolded sparse coding. In *Advances in Neural Information Processing Systems 32*, pages 13100–13110. Curran Associates, Inc., 2019.
- D. P. Bertsekas. *Nonlinear Programming*. Athena Scientific, 1995.
- M. Borgerding, P. Schniter, and S. Rangan. Amp-inspired deep networks for sparse linear inverse problems. *IEEE Transactions on Signal Processing*, 65(16):4293–4308, 2017.
- A. Cauchy. Méthode générale pour la résolution des systèmes d'équations simultanées. *Comp. Rend. Sci. Paris*, 25(1847):536–538, 1847.
- X. Chen, J. Liu, Z. Wang, and W. Yin. Theoretical linear convergence of unfolded ista and its practical weights and thresholds. In *Advances in Neural Information Processing Systems*, pages 9061–9071, 2018.
- D. Dua and C. Graff. UCI machine learning repository, 2017.
- R. Fletcher. *Practical methods of optimization*. John Wiley & Sons, 2013.
- G. E. Forsythe. On the asymptotic directions of the-dimensional optimum gradient method. *Numerische Mathematik*, 11(1):57–76, 1968.
- G. H. Golub and M. D. Kent. Estimates of Eigenvalues for Iterative Methods. *Mathematics of Computation*, 53(188):619, 1989.
- K. Gregor and Y. LeCun. Learning fast approximations of sparse coding. In *Proceedings of the 27th International Conference on International Conference on Machine Learning*, pages 399–406. Omnipress, 2010.
- H. He, C.-K. Wen, S. Jin, and G. Y. Li. A model-driven deep learning network for mimo detection. In *2018 IEEE Global Conference on Signal and Information Processing (GlobalSIP)*, pages 584–588. IEEE, 2018.
- J. R. Hershey, J. L. Roux, and F. Weninger. Deep unfolding: Model-based inspiration of novel deep architectures. *arXiv preprint arXiv:1409.2574*, 2014.
- A. E. Hoerl and R. W. Kennard. Ridge regression: Biased estimation for nonorthogonal problems. *Technometrics*, 12(1):55–67, 1970.
- L. Hogben. *Handbook of linear algebra*. Chapman and Hall/CRC, 2013.
- D. Ito, S. Takabe, and T. Wadayama. Trainable ista for sparse signal recovery. *IEEE Transactions on Signal Processing*, 67(12):3113–3125, 2019.
- K. H. Jin, M. T. McCann, E. Froustey, and M. Unser. Deep convolutional neural network for inverse problems in imaging. *IEEE Transactions on Image Processing*, 26(9):4509–4522, 2017.
- U. S. Kamilov and H. Mansour. Learning optimal nonlinearities for iterative thresholding algorithms. *IEEE Signal Processing Letters*, 23(5):747–751, 2016.
- M. Kellman, E. Bostan, N. Repina, and L. Waller. Physics-based learned design: Optimized coded-illumination for quantitative phase imaging. *IEEE Transactions on Computational Imaging*, 2019.
- D. P. Kingma and J. Ba. Adam: A method for stochastic optimization. *arXiv preprint arXiv:1412.6980*, 2014.
- L. Lessard, B. Recht, and A. Packard. Analysis and design of optimization algorithms via integral quadratic constraints. *SIAM Journal on Optimization*, 26(1):57–95, 2016.
- J. Liu, X. Chen, Z. Wang, and W. Yin. Alista: Analytic weights are as good as learned weights in lista. In *International Conference on Learning Representations*, 2019.

- [22] M. Mardani, Q. Sun, D. Donoho, V. Petyan, H. Monajemi, S. Vasanawala, and J. Pauly. Neural proximal gradient descent for compressive imaging. In *Advances in Neural Information Processing Systems*, pages 9573–9583, 2018.
- [23] M. Mardani, Q. Sun, V. Petyan, S. Vasanawala, J. Pauly, and D. Donoho. Degrees of freedom analysis of unrolled neural networks. *arXiv preprint arXiv:1906.03742*, 2019.
- [24] J. C. Mason and D. C. Handscomb. *Chebyshev polynomials*. Chapman and Hall/CRC, 2002.
- [25] C. Metzler, A. Mousavi, and R. Baraniuk. Learned d-amp: Principled neural network based compressive image recovery. In *Advances in Neural Information Processing Systems*, pages 1772–1783, 2017.
- [26] V. Monga, Y. Li, and Y. C. Eldar. Algorithm unrolling: Interpretable, efficient deep learning for signal and image processing. *arXiv preprint arXiv:1912.10557*, 2019.
- [27] E. Nachmani, Y. Be'ery, and D. Burshtein. Learning to decode linear codes using deep learning. In *2016 54th Annual Allerton Conference on Communication, Control, and Computing (Allerton)*, pages 341–346. IEEE, 2016.
- [28] Y. Nesterov. Introductory lectures on convex programming volume i: Basic course. *Lecture notes*, 3(4):5, 1998.
- [29] A. Paszke, S. Gross, F. Massa, A. Lerer, J. Bradbury, G. Chanan, T. Killeen, Z. Lin, N. Gimelshein, L. Antiga, A. Desmaison, A. Kopf, E. Yang, Z. DeVito, M. Raison, A. Tejani, S. Chilamkurthy, B. Steiner, L. Fang, J. Bai, and S. Chintala. Pytorch: An imperative style, high-performance deep learning library. In H. Wallach, H. Larochelle, A. Beygelzimer, F. d'Alché-Buc, E. Fox, and R. Garnett, editors, *Advances in Neural Information Processing Systems 32*, pages 8024–8035. Curran Associates, Inc., 2019.
- [30] B. T. Polyak. Some methods of speeding up the convergence of iteration methods. *USSR Computational Mathematics and Mathematical Physics*, 4(5):1–17, 1964.
- [31] M. Redmond and A. Baveja. A data-driven software tool for enabling cooperative information sharing among police departments. *European Journal of Operational Research*, 141(3):660–678, 2002.
- [32] D. E. Rumelhart, G. E. Hinton, and R. J. Williams. Learning representations by back-propagating errors. *Nature*, 323(6088):533–536, Oct 1986.
- [33] N. Samuel, T. Diskin, and A. Wiesel. Deep mimo detection. In *2017 IEEE 18th International Workshop on Signal Processing Advances in Wireless Communications (SPAWC)*, pages 1–5. IEEE, 2017.
- [34] W. Shi, F. Jiang, S. Zhang, and D. Zhao. Deep networks for compressed image sensing. In *2017 IEEE International Conference on Multimedia and Expo (ICME)*, pages 877–882. IEEE, 2017.
- [35] P. Sprechmann, A. M. Bronstein, and G. Sapiro. Learning efficient sparse and low rank models. *IEEE transactions on pattern analysis and machine intelligence*, 37(9):1821–1833, 2015.
- [36] S. Takabe, M. Imanishi, T. Wadayama, R. Hayakawa, and K. Hayashi. Trainable projected gradient detector for massive overloaded mimo channels: Data-driven tuning approach. *IEEE Access*, 7:93326–93338, 2019.
- [37] T. Wadayama and S. Takabe. Deep learning-aided trainable projected gradient decoding for LDPC codes. In *IEEE International Symposium on Information Theory, ISIT 2019, Paris, France, July 7-12, 2019*, pages 2444–2448, 2019.
- [38] B. Xin, Y. Wang, W. Gao, D. Wipf, and B. Wang. Maximal sparsity with deep networks? In *Advances in Neural Information Processing Systems*, pages 4340–4348, 2016.
- [39] M. Yao, J. Dang, Z. Zhang, and L. Wu. Sure-tista: A signal recovery network for compressed sensing. In *ICASSP 2019-2019 IEEE International Conference on Acoustics, Speech and Signal Processing (ICASSP)*, pages 3832–3836. IEEE, 2019.
- [40] J. Zhang and B. Ghanem. Ista-net: Interpretable optimization-inspired deep network for image compressive sensing. In *Proceedings of the IEEE Conference on Computer Vision and Pattern Recognition*, pages 1828–1837, 2018.